Summer Rainfall Variability in Low-Latitude Highlands of China and Subtropical Indian Ocean Dipole

JIE CAO

Department of Atmospheric Sciences, Yunnan University, and Yunnan Key Laboratory of International Rivers and Transboundary Eco-Security, Kunming, China

PING YAO

Department of Atmospheric Sciences, Yunnan University, and Department of Environmental Science and Engineering, Southwest Forestry University, Kunming, China

LIN WANG

Center for Monsoon System Research, Institute of Atmospheric Physics, Chinese Academy of Sciences, Beijing, China

KUI LIU

Department of Atmospheric Sciences, Yunnan University, and Yunnan Key Laboratory of International Rivers and Transboundary Eco-Security, Kunming, China

(Manuscript received 18 February 2013, in final form 19 August 2013)

ABSTRACT

Based on reanalysis and observational datasets, this study proposes a reasonable mechanism for summer rainfall variations over the low-latitude highlands (LLH) of China, in which a subtropical Indian Ocean dipole (SIOD)-like pattern is the key external thermal forcing. In summers with a positive SIOD-like pattern, sea surface temperature (SST) anomalies may lead to lower-tropospheric divergence over the tropical Indian Ocean and convergence over the subtropical southwestern Indian Ocean and Arabian Sea. The convergence over the Arabian Sea can induce easterly anomalies of the divergent wind component off the eastern coast of the Bay of Bengal (BOB), while the divergence over the tropical Indian Ocean can change the interhemispheric vertical circulation and produce a descending motion over the same area and cyclonic anomalies in the rotational wind component over the Indian peninsula. The combined effect of the divergent and rotational wind anomalies and enhanced interhemispheric vertical circulation facilitates easterly anomalies and weakens climatological water vapor flux to the northern BOB. Therefore, anomalous water vapor divergence and less precipitation are observed over the LLH. In summers with a negative SIOD-like pattern, the situation is approximately the same but with opposite polarity and a weaker role of the divergent wind component. Further analyses indicate that the summertime SIOD-like pattern can be traced to preceding seasons, especially in positive SIOD-like years. The SST–wind–evaporation feedback mechanism could account for maintenance of the SIOD-like pattern. These results provide efficient prediction potential for summer rainfall variations over the LLH.

1. Introduction

Low-latitude highlands (LLH) are areas where the average altitude exceeds 1500 m above sea level, below 30°N latitude (e.g., Tao et al. 2013). In China, LLH include Yunnan, southern Sichuan, western Guizhou, and western Guangxi Provinces. The geographic location of this area is unique (Fig. 1), with the Bay of Bengal (BOB) to its southwest, South China Sea (SCS) to its southeast, and Tibetan Plateau to its northwest. Terrain in this area is very complex, highest in the northwest and lowest in the southeast, which leads to a diverse climate ranging from tropical to temperate. The climate is characterized by distinct rainy and dry seasons (e.g., Qin et al. 1997). In the main rainy season from June to August (Fig. 2), the interface between the Indian and East Asian

Corresponding author address: Dr. Jie Cao, Department of Atmospheric Sciences, Yunnan University, Kunming 650091, China. E-mail: caoj@ynu.edu.cn

DOI: 10.1175/JCLI-D-13-00121.1

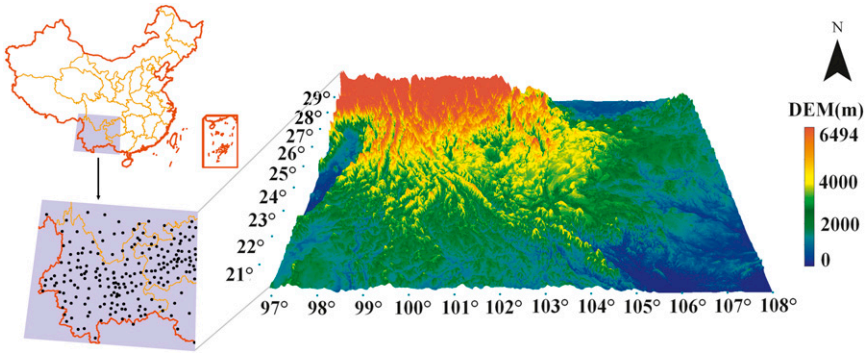

FIG. 1. Location and terrain of low-latitude highlands in China. Rainfall stations are indicated by black dots.

summer monsoons is in the area and contributes to substantial climate variability (Cao et al. 2012). Droughts and floods are widespread and frequent in the LLH. Their associated economic losses can reach about 70% of all meteorological disasters (Qin et al. 1997; Cheng et al. 2009). For example, severe droughts were observed continuously in the area during 2010 (e.g., Barriopedro et al. 2012; Yang et al. 2012), 2011 (e.g., Sun and Yang 2012), and 2012 (e.g., NCC/CMA 2012) (Fig. 2). These droughts had significant impacts on economic growth and the daily lives of millions of people. The severity of these hazards attracts the attention of both the public and scientists. It is therefore urgent and valuable to understand the possible causes and mechanism of these hazards.

Compared with fruitful studies about droughts and floods in eastern China, such as in the Yangtze–Huaihe River valley (e.g., Tao and Chen 1987; Chen 2002; Ding and Chan 2005; Chen et al. 2006; Huang et al. 2012a; Ma et al. 2011, 2012), there has been relatively little research on the mechanism of drought and flood occurrence in the LLH. A possible reason is that climate variability in that area is very different from that in eastern China, which makes associations difficult (e.g., Qin et al. 1997; Liu et al. 2011). For example, severe droughts in Yunnan Province from autumn 2009 through spring 2010 were suggested to be caused by numerous factors. These included anomalous disturbances in the westerly belt (Yang et al. 2012), negative phases of the North Atlantic Oscillation (Song et al. 2011) and Arctic Oscillation (Huang et al. 2012b), persistent anomalies of the Madden–Julian oscillation (Lü et al. 2012), and a weakened broad-scale South Asian summer monsoon (Barriopedro et al. 2012).

Limited statistical studies indicate that spring and summer droughts in the LLH are associated with continuous strengthening and stable westward expansion of the western Pacific subtropical high, weakening and westward shift of the monsoon low, weaker meridional water vapor transport from the BOB, and active convection around Sumatra (Yan et al. 1994; Xie et al. 2005; Li et al. 2008; Yang et al. 2011; Wang et al. 2012). In contrast, relationships between atmospheric external forcing and droughts were not well established. Liu et al. (2011) pointed out that most regions of Yunnan Province had above normal summer precipitation during the developing stage of La Niña, with only marginal summer precipitation anomalies observed in other stages of El Niño–Southern Oscillation (ENSO). However, the confidence level in Liu et al. (2011) was not very high. Moreover, their study cannot explain recent droughts in the LLH. For example, the sea surface temperature (SST) monitor shows that La Niña was in a developing phase when the 2010/11 and 2011/12 droughts occurred (http://www.cpc.ncep.noaa.gov/products/analysis_monitoring/ensostuff/ensoyears.shtml), contrary to the conclusion of Liu et al. (2011). Moreover, El Niño was in a developing phase during the 2009/10 droughts. These results suggest that the rainy season droughts of 2009–11 in the LLH cannot be substantially accounted for by SST anomalies over the tropical Pacific.

Nevertheless, some studies indicate that early summer rainfall in Yunnan Province changes significantly when

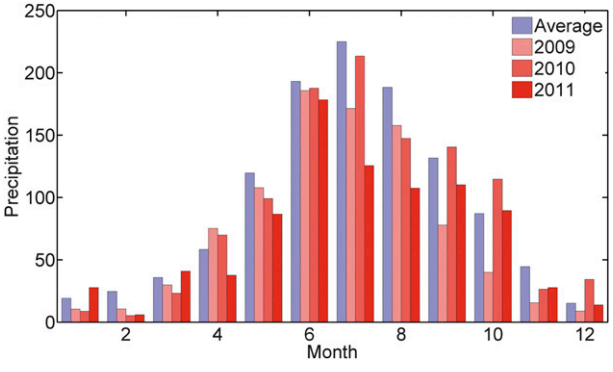

FIG. 2. Annual cycle of monthly rainfall averaged over LLH, from climatology and years 2009, 2010, and 2011 (mm).

SST anomalies are present over both the Pacific and Indian Oceans (Yan et al. 2005; Yang et al. 2011). This implies a role for the Indian Ocean in affecting LLH rainfall. Further, many recent studies suggest that this ocean can strongly influence the East Asian summer climate in a manner different from ENSO (e.g., Yang et al. 2007; Xie et al. 2009; Huang et al. 2010; Wang and Wu 2012). Therefore, it is meaningful to investigate the potential role of the Indian Ocean in summer rainfall variations of the LLH.

The subtropical Indian Ocean dipole (SIOD) is an important ocean–atmosphere phenomenon in the southern Indian Ocean. It is characterized by an SST seesaw, in which the southwestern Indian Ocean is warmer (or colder) than its eastern part (Behera and Yamagata 2001; Morioka et al. 2012). The SIOD significantly influences climate variability around that ocean. For example, Reason (2001) indicated that a positive SIOD can generate more summer rainfall over large parts of southeastern Africa by strengthening the convergence of moist air generated over the warm southwestern Indian Ocean. Terray et al. (2003) suggested that a strong (weak) Indian summer monsoon is preceded by a significant positive (negative) SIOD via positive dynamical feedback between the Mascarene high and underlying SST anomalies during boreal winter. Jia and Li (2005) proposed that with the SIOD positive phase, the western Pacific subtropical high extends westward and the Tibetan high is strong and located eastward. This leads to more (less) rainfall in the Yangtze River basin (South China). The LLH is northeast of the Indian Ocean and is possibly influenced by its variability, including the SIOD. Moreover, some studies reveal that the SIOD phase is independent of the simultaneous ENSO phase (e.g., Fauchereau et al. 2003; Washington and Preston 2006; Huang and Shukla 2007), implying the SIOD as an independent forcing of LLH rainfall. Therefore, we explore here whether the SIOD can influence LLH summer rainfall and, if so, how this influence is established.

Datasets and methods are described in section 2. Section 3 investigates the relationship between rainfall anomalies in the LLH and the SIOD-like SST pattern. Section 4 describes the possible mechanism through which the SIOD-like pattern impacts LLH summer rainfall. In section 5, the prediction potential of the SIOD-like pattern and the corresponding physical processes that enable the SIOD-like pattern to persist from preceding seasons to summer are revealed through composite analysis. Finally, a summary and discussion are in section 6.

2. Data and methods

The atmospheric data used are from the monthly-mean Modern-Era Retrospective Analysis for Research and Applications (MERRA) dataset, provided by the Global Modeling and Assimilation Office (GMAO) and Goddard Earth Sciences Data and Information Services Center (GES DISC) (Rienecker et al. 2011). This dataset has 1.25° by 1.25° horizontal resolution and spans the period 1979–present. The oceanic data used are from the monthly-mean Hadley Centre Global Sea Ice and SST (HadISST) dataset (version 1.1), provided by the Met Office Hadley Centre. It has 1.0° by 1.0° horizontal resolution and covers the period 1870–present (Rayner et al. 2003). Monthly-mean station observation data are from the Chinese Meteorological Data Center and Climate Center of Yunnan Province, taken from 209 stations across the LLH (21°–29°N, 97°–108°E) (Fig. 1). These observation data begin in 1961 and are updated every month.

Singular value decomposition (SVD) is used to identify major covariation modes between LLH summer rainfall and potential driving factors (Bretherton et al. 1992). Composite and correlation analyses are used to reveal associated climatic anomalies. To identify statistically significant patterns from random noise, experiments with Gaussian-distributed random data were repeated 100 times, and variance contribution rates of the singular values at a significance level of 95% were obtained via the Monte Carlo method (Shen and Lau 1995). Herein, summer refers to the average of June–August (JJA). The time period examined is from 1979 to 2011.

3. Association of LLH rainfall with Indian Ocean SST

The SVD analysis is used to reveal the association between LLH summer rainfall and possible driving factors. One input field for SVD is the station rainfall in the LLH (Fig. 1), and the other is a combination of summer-mean SST and 925-hPa winds over the Indian Ocean (40°S–30°N, 35°–110°E). Such a combination of SST and lower-tropospheric wind has been proven efficient in identifying atmosphere–ocean coupling modes associated with LLH rainfall (e.g., Wang et al. 2003). The first five SVD modes exceed the noise level (not shown), and the first mode explains 24.8% of total covariance. It is significantly larger than, and separated from, the other modes. In the following, we focus on this first SVD mode.

Figure 3a shows that the first SVD mode of summer rainfall has a clear monopole structure over the LLH. Positive centers with values exceeding 60 units are mainly in the central and western LLH (around 21°–29°N, 100°–104°E, and 21°–25°N, 105°–108°E) and in small regions of the northeastern LLH (around 26°–28°N, 106°–108°E).

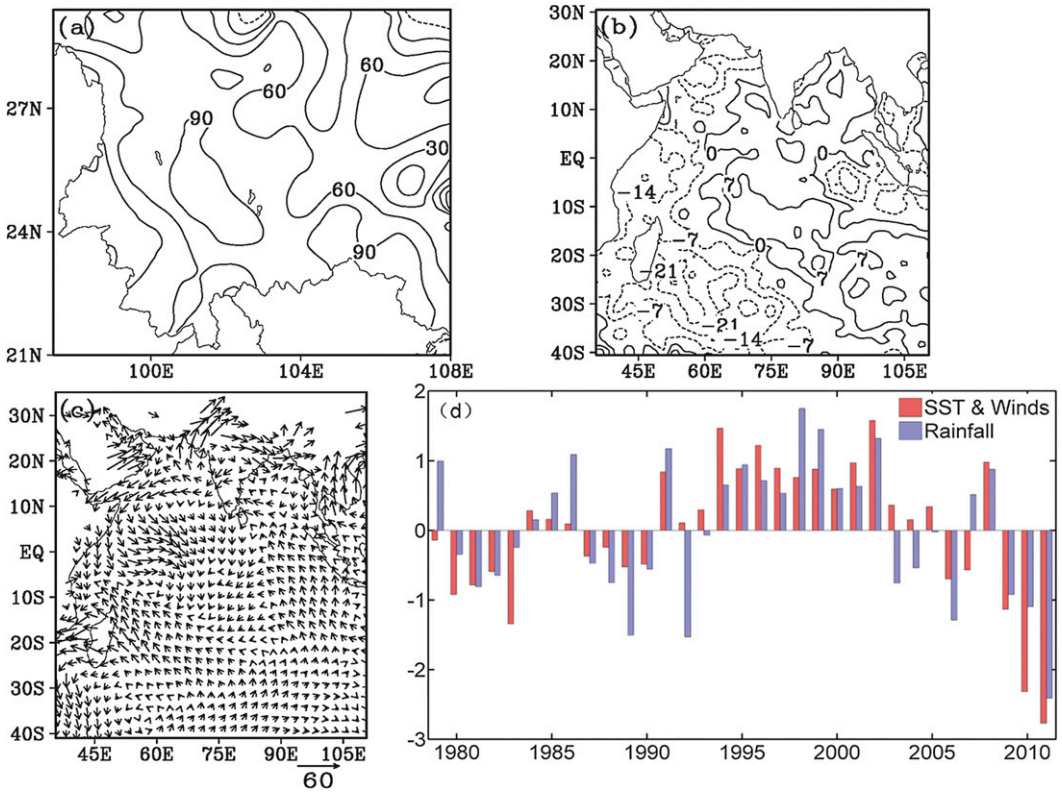

FIG. 3. First mode of SVD for (a) summer rainfall over LLH, (b) SST, and (c) winds at 925 hPa. (d) Time coefficients of first mode.

Such a spatial pattern suggests that the first SVD modes capture the intensity of LLH summer rainfall. Regarding the associated simultaneous SST mode, the most prominent anomalies are over the southern Indian Ocean, with negative (positive) centers exceeding 14 (7) units over the southwestern (southeastern) parts of that ocean (Fig. 3b). This northwest–southeast orientation resembles the SIOD (e.g., Behera and Yamagata 2001). Corresponding to the SIOD-like SST anomalies, two pairs of cyclonic and anticyclonic anomalies are observed at 925 hPa. One is located over the southwestern Indian Ocean (40°S–0°, 30°–90°E) and the other is located over the northwestern Indian Ocean (0°–20°N, 50°–80°E) (Fig. 3c).

The correlation coefficient between the time series of combined SST and 925-hPa winds and that of LLH rainfall (Fig. 3d) is 0.75, exceeding the 99.9% confidence level. These results suggest that the SIOD-like SST anomalies are closely associated with and may be important to LLH summer rainfall variability. When the SIOD-like pattern is in the negative phase, that is, when SST over the southwestern (southeastern) Indian Ocean is lower (higher) than normal, LLH summer rainfall tends to be abundant and vice versa. Such a relationship is likely established through the two pairs of anomalous gyres over the western Indian Ocean. In the following sections, composite analysis is used to confirm the results obtained by SVD and to depict the corresponding physical process by which the SIOD-like SST pattern influences LLH summer rainfall.

To confirm the robustness of results obtained by SVD, we further calculated the correlation coefficients between average LLH summer rainfall and corresponding SST over the Indian Ocean and Pacific (Fig. 4). It reveals that the correlation pattern is similar to Fig. 3b over the Indian Ocean. Significant correlation can also be observed over the South Pacific, but it is different from the SST pattern of conventional ENSO. These correlation results imply that the SIOD-like SST pattern over the Indian Ocean may exert more significant influences on LLH summer rainfall than ENSO does.

4. Possible mechanism

To investigate the influence of the SIOD-like SST pattern on LLH summer rainfall and associated processes, a composite analysis was performed based on the normalized time series of the first SVD mode for the

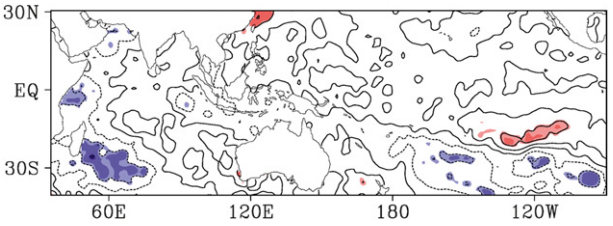

FIG. 4. Correlation coefficient between the averaged summer (JJA) rainfall over LLH and the simultaneous SST. Light and dark shading indicate 90% and 95% confidence levels, respectively.

combined SST and 925-hPa winds (red bars in Fig. 3d). For clarity, if SST over the southwestern Indian Ocean is higher (lower) than normal, and that over the southeastern ocean is lower (higher) than normal during summer of a given year, that year is called a positive (negative) SIOD-like year. Based on a criterion of ±0.5 standard deviation, 10 (11) out of 33 years were identified as positive (negative) SIOD-like years. These years are 1980, 1981, 1982, 1983, 1989, 2006, 2007, 2009, 2010, and 2011. The 11 negative years are 1991, 1994, 1995, 1996, 1997, 1998, 1999, 2000, 2001, 2002, and 2008.

a. Rainfall

Figure 5 shows composite anomalies of LLH summer rainfall according to the polarity of the SIOD-like pattern. In summers with a positive pattern, rainfall is significantly below normal over most of the LLH, with maximum rainfall anomalies exceeding 200 mm in an absolute sense (Fig. 5a). Further analysis indicates that 73 (103) out of the 209 stations, or 34.9% (49.3%), exceeded the 95% (90%) confidence level from the Monte Carlo test. In summers with a negative SIOD-like pattern, rainfall was significantly above normal over most of the LLH, with maximum rainfall anomalies exceeding 150 mm (Fig. 5b). The area passing the significance test is larger than that for the positive phase. There were 109 (129) stations, or 52.2% (61.7%) of the total, that exceeded the 95% (90%) confidence level. To our knowledge, these results are the best ever reported for variations of LLH summer rainfall. The two anomalous patterns in Fig. 5 resemble the SVD map of rainfall to a high degree (Fig. 3a). The strong correspondence between the composite analysis results and that of SVD suggests that the relationship between the SIOD-like pattern and LLH summer rainfall is reliable.

b. Lower-tropospheric winds and column-integrated water vapor transport

The rainfall changes could be caused by related circulation anomalies. During summers with a positive SIOD-like pattern, there was an anomalous cyclone over the BOB. Clear lower-tropospheric easterly anomalies associated with this cyclone were over the northern BOB (Fig. 6a). In a climatological-mean sense, southwesterly winds prevail over the northern BOB and serve as a major water vapor source for the LLH. Therefore, the aforesaid easterly anomalies imply that the moisture supply from the BOB to the LLH is significantly declined, which favors less precipitation in the latter area. Inspection of column-integrated water vapor flux (integrated from the surface to 200 hPa) and its divergence confirm this interpretation. The water vapor flux features an anomalous cyclone over the BOB. Correspondingly, there are significant westward water vapor flux anomalies over the northern BOB and northern Indochinese peninsula (Fig. 6b), resembling the anomalous wind pattern. This configuration leads to anomalous water vapor divergence over the LLH and anomalous water vapor convergence over the BOB (Fig. 6c), generating less summer rainfall over the LLH. In contrast, during summers with a negative SIOD-like pattern, an anomalous anticyclone dominates the BOB. Clear westerly anomalies related to this anticyclone are found in the northern BOB (Fig. 6d). Associated water vapor flux and divergence anomalies over the northern BOB and

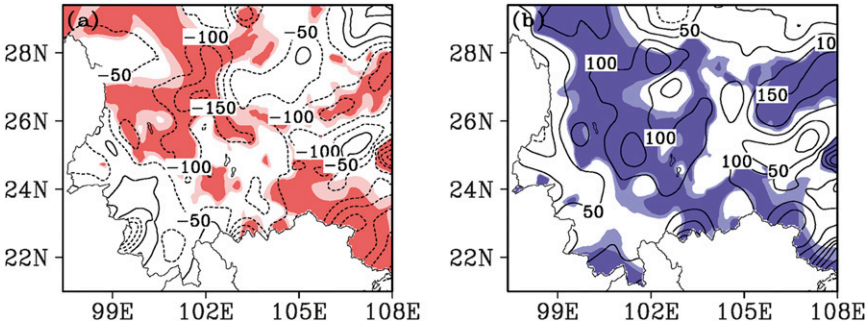

FIG. 5. Composite anomalies of summer (JJA) rainfall during (a) positive SIOD-like years and (b) negative SIOD-like years. Contour intervals are 50 mm. Light and dark shading indicate 90% and 95% confidence levels, respectively. See text for the years used in composite.

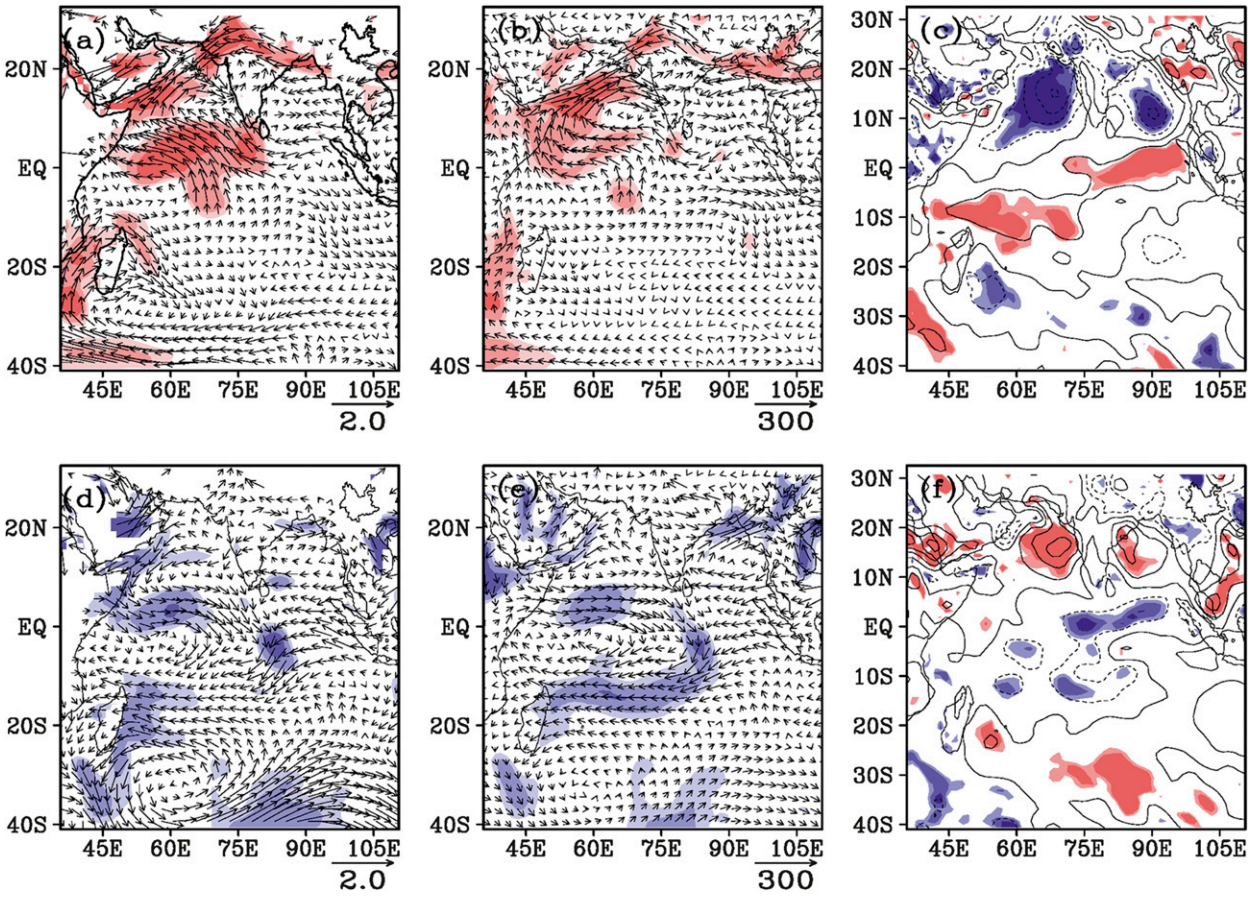

FIG. 6. Composite anomalies of summer (JJA) mean (a) 925-hPa winds ($m\,s^{-1}$), (b) column-integrated water vapor flux ($kg\,m^{-1}\,s^{-1}$), and (c) divergence of water vapor flux (contour interval = $3 \times 10^{-5}\,kg\,m^{-2}\,s^{-1}$) in positive SIOD-like years. (d)–(f) As in (a)–(c), but for negative SIOD-like years. Light and dark shading indicate 90% and 95% confidence levels, respectively.

Indochinese peninsula are roughly opposite those during summers with a positive SIOD-like pattern (Figs. 6e,f). Therefore, enhanced water vapor divergence over the BOB and increased water vapor convergence over the LLH favor more summer rainfall over the latter area.

The anomalous circulations over the BOB (especially the zonal wind anomalies and associated changes of water vapor flux in the northern BOB) are likely the important factors for LLH rainfall variations. To understand the formation of these wind anomalies, the wind is decomposed into divergent and rotational components. In summers with a positive SIDO-like pattern, lower-tropospheric divergent wind fields are featured, with apparent convergence zones over the southwestern Indian Ocean (around 25°S, 60°E) and northern Arabian Sea (around 15°N, 65°E) (Fig. 7a). There is a third convergence zone in the central BOB (around 15°N, 85°E). To the east of this zone are significant easterly anomalies (Fig. 7a). In the rotational wind fields, two pairs of cyclonic and anticyclonic anomalies appear. One pair is from south of Madagascar to the western tropical Indian Ocean in the Southern Hemisphere, and the other is from the southern Arabian Sea to the northwestern Indian peninsula in the Northern Hemisphere (Fig. 7b). The two anomalous anticyclones, over the western tropical Indian Ocean in both hemispheres, suggest that the Mascarene high and low-level cross-equatorial gyre over the tropical Indian Ocean, which links the monsoon trough to the Mascarene high at the surface, shift to the north of their normal positions during boreal summers with a positive SIOD-like pattern. Accompanied by the northward-shifted Mascarene high and low-level cross-equatorial gyre, an enhanced interhemispheric vertical circulation appears, with an ascending branch over the BOB and descending one over the tropical southern Indian Ocean (Fig. 6c). The cyclonic anomaly over the Indian peninsula corresponds to anomalous easterlies in the northern BOB. Hence, the divergent winds, rotational winds, and interhemispheric vertical circulation contribute positively to the anomalous easterlies over the northern BOB.

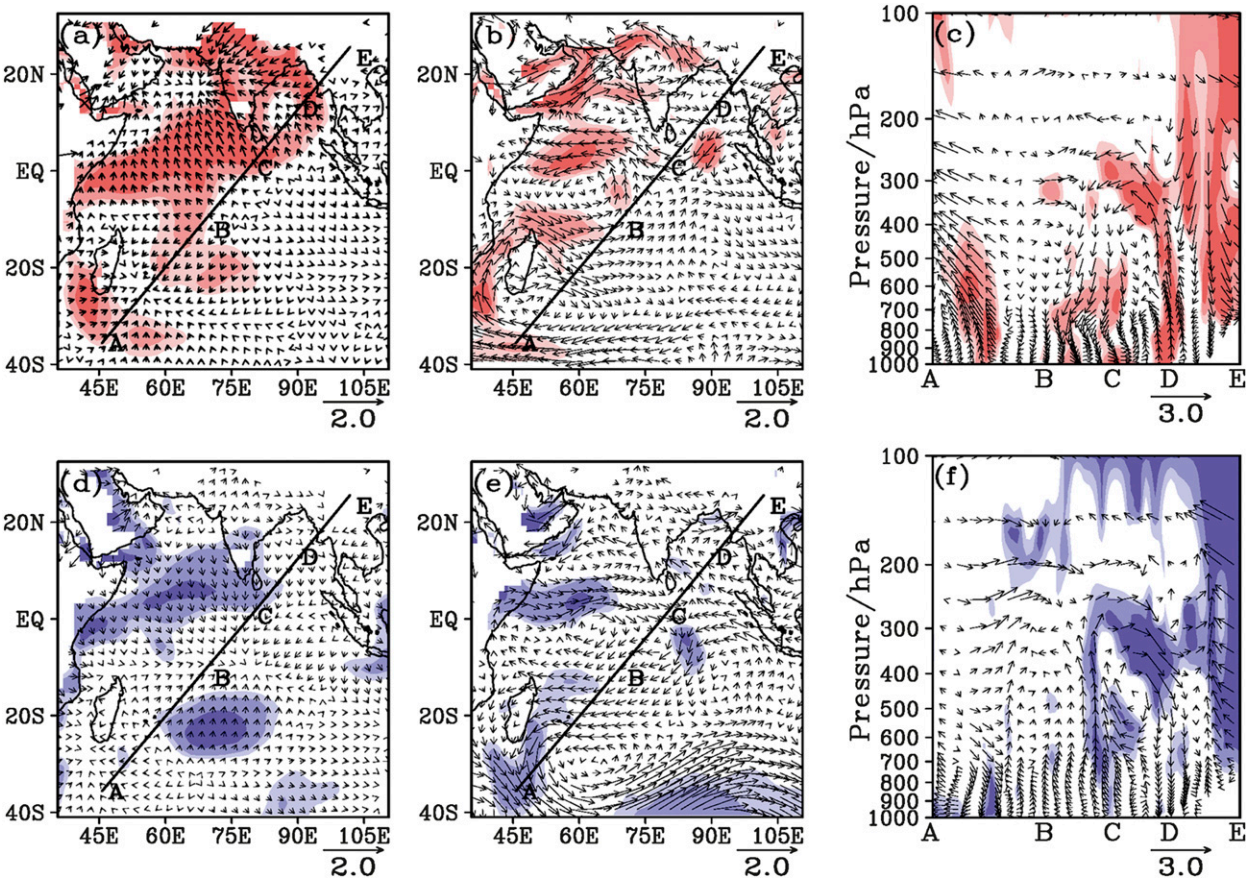

FIG. 7. Composite anomalies of summer (JJA) mean (a) divergent winds at 925 hPa ($m\,s^{-1}$), (b) rotational winds at 925 hPa ($m\,s^{-1}$), and (c) vertical circulation along line ABCDE ($m\,s^{-1}$; vertical speeds are multiplied by 100 for visual clarity) in positive SIOD-like years. (d)–(f) As in (a)–(c), but for negative SIOD-like years. Light and dark shading indicate 90% and 95% confidence levels, respectively.

During summers with a negative SIOD-like pattern, lower-tropospheric divergence is observed over the subtropical southern Indian Ocean (around 25°S, 70°E) and the tropical northern Indian Ocean (around 15°N, 65°E), while there is convergence around the tropical southern part of the ocean (around 10°S, 70°E) (Fig. 7d). Associated divergent winds are featured, with weak westerly anomalies over the northern BOB. The rotational wind field roughly resembles that in the positive SIOD-like summers but with opposite polarity and weaker anomalies over the Indian peninsula (Fig. 7e). This anomalous circulation configuration suggests that both the Mascarene high and low-level cross-equatorial gyre over the tropical Indian Ocean shift southward during boreal summers with a negative SIOD-like pattern. At the same time, a suppressed interhemispheric vertical circulation develops, with an anomalous descending branch over the BOB and an anomalous ascending one over the tropical southern Indian Ocean (Fig. 7f). Therefore, the divergent and rotational wind components and suppressed interhemispheric vertical circulation contribute positively to the westerly anomalies over the northern BOB. Moreover, comparison between the divergent and rotational winds indicates that the area of divergent winds exceeding the 95% confidence level is much larger than that of the rotational winds, regardless of the polarity of the SIOD-like pattern (Figs. 6a,b, 5d,e). The results from the composite analysis suggest that the three-dimensional divergent circulation anomalies forced out by the SIOD-like pattern are important in connecting the SIOD-like pattern with LLH summer rainfall.

c. *Lower-tropospheric wind removal of local precipitation effect*

Water vapor convergence/divergence is significantly enhanced over the BOB and Arabian Sea (Figs. 6c,f), indicating more/less precipitation around the Indian subcontinent. The enhanced (suppressed) precipitation may excite an anomalous cyclonic (anticyclonic) circulation

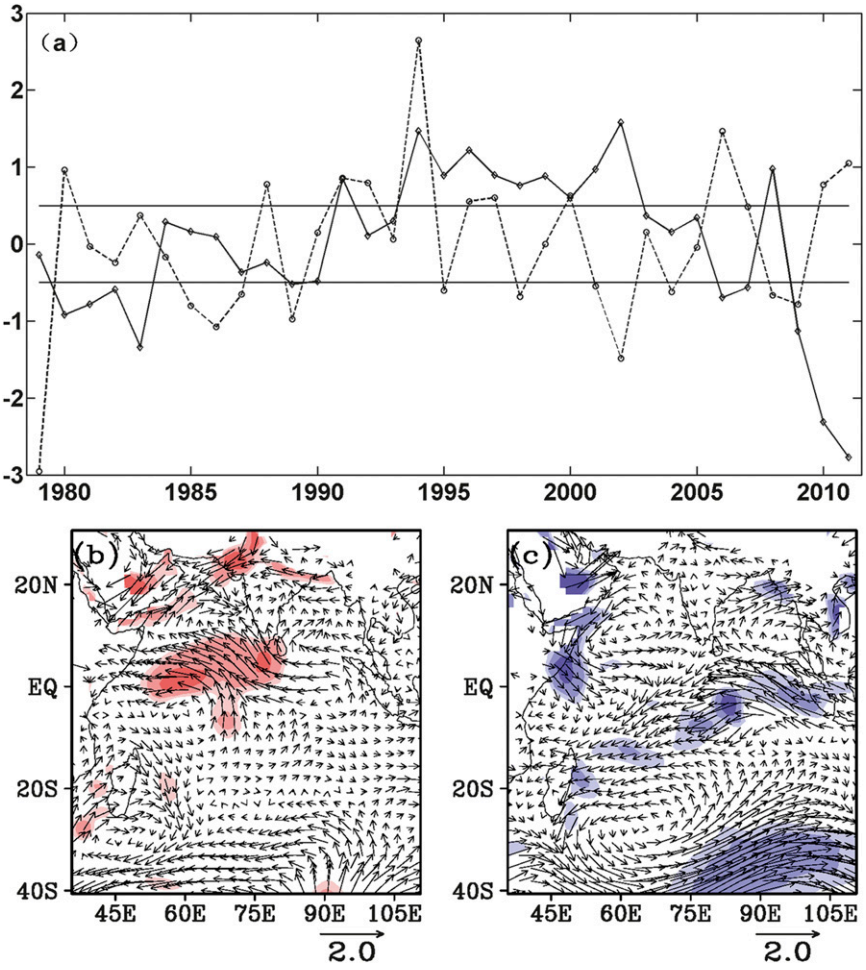

FIG. 8. (a) Normalized time coefficients of first SVD mode for combination of SST and wind fields (dashed line), and normalized precipitation index averaged over 13.75°–21.25°N, 71.25°–93.75°E (solid line). Composite anomalies of summer (JJA) mean (b) 925-hPa winds ($m\,s^{-1}$) in positive SIOD-like years with normal precipitation. (c) As in (b), but for negative SIOD-like years with normal precipitation. Light and dark shading indicate 90% and 95% confidence levels, respectively. See text for years used in composite.

in the lower troposphere and possibly contribute to the easterly/westerly anomalies over the northern BOB. Hence, one may ask whether the observed zonal wind anomalies over the northern BOB are a response to the SIOD-like pattern or to in situ precipitation anomalies around the Indian subcontinent. To answer this question, we did a composite analysis by removing potential influences of precipitation over the subcontinent. First, we constructed a precipitation index by averaging precipitation over the subcontinent (13.75°–21.25°N, 71.25°–93.75°E). Second, years in which the normalized precipitation index exceeded ±0.5 standard deviation were removed from the 10 positive and 11 negative SIOD-like years, because there is negative correlation between the normalized precipitation index and normalized time series of the first SVD mode for the combined SST and 925-hPa winds. Based on this criterion, 6 of the 10 positive SIOD-like years remained (1981, 1982, 1983, 1989, 2007, and 2009), as did 6 of the 11 negative years (1991, 1994, 1996, 1997, 1999, and 2000) (Fig. 8a).

Figures 8b and 8c show composite anomalies based on the 6 positive and 6 negative SIOD-like years. They reveal that the lower-tropospheric wind anomalies are almost identical to those in Figs. 6a and 6d. Significant lower-tropospheric westerly (easterly) anomalies can still be observed in the northern BOB during summers of positive (negative) SIOD-like patterns, even if precipitation around the Indian subcontinent and BOB (Figs. 8b,c) is normal. Hence, the westerly (easterly) anomalies in the northern Indian subcontinent and BOB are

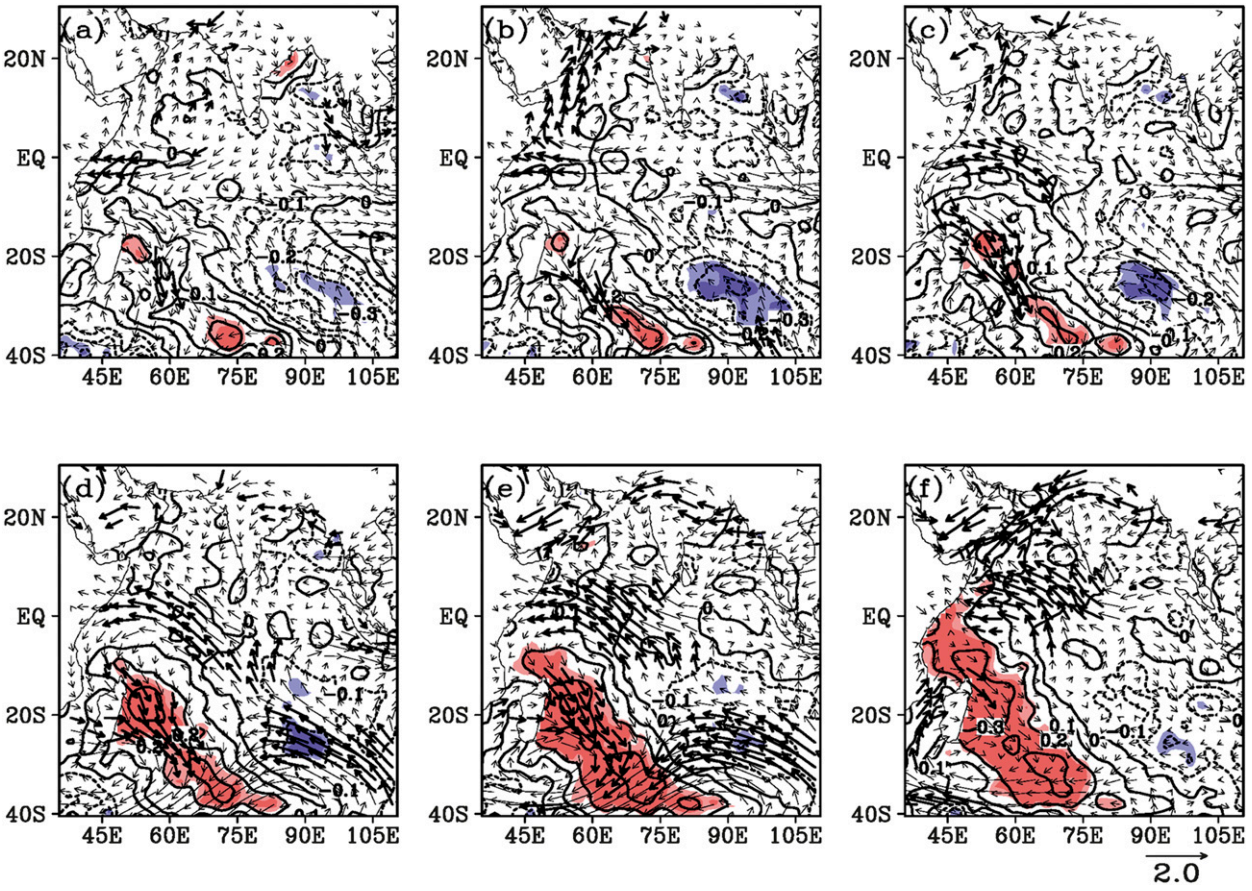

FIG. 9. Composite anomalies of 3-month average SST (contour interval = 0.1°C) and 925-hPa winds ($m\,s^{-1}$) for (a) January–March, (b) February–April, (c) March–May, (d) April–June, (e) May–July, and (f) June–August in positive SIOD-like years. Light and dark shading indicate 90% and 95% confidence levels of SST, respectively. Thick vectors represent wind exceeding 95% confidence level.

mainly a response to the SIOD-like SST pattern. Nevertheless, confidence levels of the zonal wind anomalies in the northern BOB are slightly lower in Figs. 8b and 8c than those in Figs. 6a and 6d. This suggests that the precipitation anomalies around the Indian subcontinent also contribute constructively to the zonal wind anomalies, although their role is of secondary importance. The related process may be as follows. Once an anomalous cyclonic (anticyclonic) circulation in the lower troposphere is excited by the SIOD-like SST pattern, precipitation anomalies form because of anomalous water vapor convergence and vertical atmospheric motion. The precipitation could in turn reinforce the cyclonic (anticyclonic) circulation and contribute constructively to the westerly (easterly) anomalies in the northern BOB.

5. Prediction potential and maintain mechanism of the SIOD-like pattern

The analysis in section 4 indicates that the summertime SIOD-like SST pattern is closely associated with anomalous zonal winds and water vapor fluxes over the northern BOB, which in turn influence the LLH summer rainfall variations. To further understand this pattern, it is necessary to examine in detail the evolution of SST from preceding seasons to the following summer and associated wind anomalies.

Figure 9 presents composite maps of SST anomalies from the previous winter to current summer for years with a positive SIOD-like pattern. There is a prominent dipole over the subtropical southern Indian Ocean. Warm SSTs are centered over the southwestern Indian Ocean and extend northward to the Arabian Sea. Cool water covers the eastern Indian Ocean, including the BOB, with a center around 30°S, 95°E. From winter to summer, the warm SST anomalies over the southwestern Indian Ocean amplify and extend northwestward to Somalia, with an additional area exceeding 0.2°C and the 95% confidence level (Fig. 9). Meanwhile, both intensity and confidence level of the negative SST anomalies over the southeastern Indian Ocean decrease. This implies that the positive SST center of the SIOD-like

pattern likely has greater impacts on the atmosphere in summer.

The persistence of the positive SIOD-like pattern (especially the aforementioned positive SST center) from winter to summer can be attributed to the SST–wind–evaporation feedback mechanism and oceanic advection process. In the preceding winter, there is a divergence center in the tropical central Indian Ocean (around 5°S, 80°E) with two anticyclonic anomalies, one over the Arabian Sea and the other over the southwestern Indian Ocean (Fig. 9a). According to the Gill–Matsuno mechanism, easterlies (westerlies) can be excited to the east (west) of heating and west (east) of cooling, and a pair of anticyclones associated with a Rossby wave appears on the northeastern (northwestern) and southeastern (southwestern) flanks of the heating (cooling) region (Matsuno 1966; Gill 1980). This anomalous wind field resembles the Rossby wave pattern and is likely a response to the positive SST anomalies in the subtropical southwestern Indian Ocean and negative SST anomalies in the subtropical southeastern part of that ocean. Climatological-mean winds over the subtropical southern Indian Ocean are easterly; hence, the associated anomalous northwesterlies (southeasterlies) over the warm (cold) SST of the southwestern (southeastern) part of that ocean (Fig. 9a) reduce (enhance) the climatological-mean wind and surface evaporation. This in turn helps maintain and amplify the in situ positive (negative) SST anomalies. The anomalous northwesterlies (southeasterlies) over the southwestern (southeastern) Indian Ocean can transport warm (cold) water from the equatorial region (midlatitudes), which also contributes to the maintenance of the positive SIOD-like pattern. These two mechanisms operate from winter to summer, since the climatological-mean winds over the subtropical southern Indian Ocean are always easterly. Therefore, the positive SIOD-like pattern can persist from winter to summer (Fig. 9).

Accompanying the positive SIOD-like pattern, an anticyclonic anomaly to the northeast of Madagascar also persists from winter to summer (Fig. 9). This persistent anomalous anticyclone favors the Mascarene high and low-level cross-equatorial gyre over the tropical Indian Ocean shifting northward in boreal summer. Associated with that anticyclone, an enhanced interhemispheric vertical circulation is established, with anomalous divergence and counterpart convergence over the tropical Indian Ocean (around 10°S, 75°E; i.e., point B in Fig. 7) and region from the northern Indian subcontinent to northern BOB (around 20°N, 70°–90°E), respectively (Fig. 7). The combined effects of all the divergent and rotational wind anomalies and enhanced interhemispheric vertical circulation favor easterly anomalies in the northern BOB (Figs. 6a,b) and therefore contribute positively to the reduced water vapor flux to the LLH (Figs. 6b,c) and less precipitation there (Fig. 5a).

In negative SIOD-like years, the SST dipole is not very strong before spring (Figs. 10a,c) and becomes evident beginning in early summer (Figs. 10d,f). The amplification of the SST dipole from spring (Fig. 10c) to early summer (Fig. 10d) can also be attributed to the SST–wind–evaporation mechanism, since the anomalous southeasterly (northwesterly) winds over the southwestern (southeastern) Indian Ocean strengthen (weaken) the climatological-mean wind and associated evaporation. This facilitates in situ negative (positive) SST anomalies. The transport of cold (warm) water from midlatitudes (equatorial regions) may also contribute to the negative (positive) SST anomalies southeast of Madagascar (over the tropical southeastern Indian Ocean, around 15°S, 85°E). In summer, the positive SST anomalies in the tropical Indian Ocean favor lower-tropospheric convergence (Fig. 7d) by enhancing tropical convection. This could in turn suppress the interhemispheric vertical circulation (Fig. 7f) and form anticyclonic anomalies over the BOB (Fig. 7e). However, the negative SST anomalies off the coast of Sumatra may also contribute to the anticyclone over the BOB, via the Gill–Matsuno mechanism. Therefore, there are westerly anomalies in the northern BOB (Figs. 5d, 6d,e), which foster water vapor flux to the LLH (Figs. 6e,f) and increased precipitation there (Fig. 5b).

6. Summary and discussion

The mechanism for LLH summer rainfall variations is a difficult topic, given the complex topography and interface between the Indian and East Asian summer monsoons there (Cao et al. 2012). Although some studies suggest that ENSO could influence summer rainfall extremes in the LLH (e.g., Liu et al. 2011), areas with significant rainfall changes are limited, and corresponding statistical significance is not very high (only passing the 90% confidence level). Moreover, the recent consecutive summer droughts in 2009, 2010, and 2011 cannot be explained by ENSO because the droughts occurred in both El Niño and La Niña years.

Based on atmospheric variables from the MERRA reanalysis dataset, SST from the HadISST dataset, and observed rainfall from Chinese weather stations, this study identified a close relationship between the SIOD-like pattern and LLH summer rainfall variations. During positive SIOD-like summers, that is, SST anomalies below (above) normal in the southeastern (southwestern) Indian Ocean, anticyclonic anomalies are excited

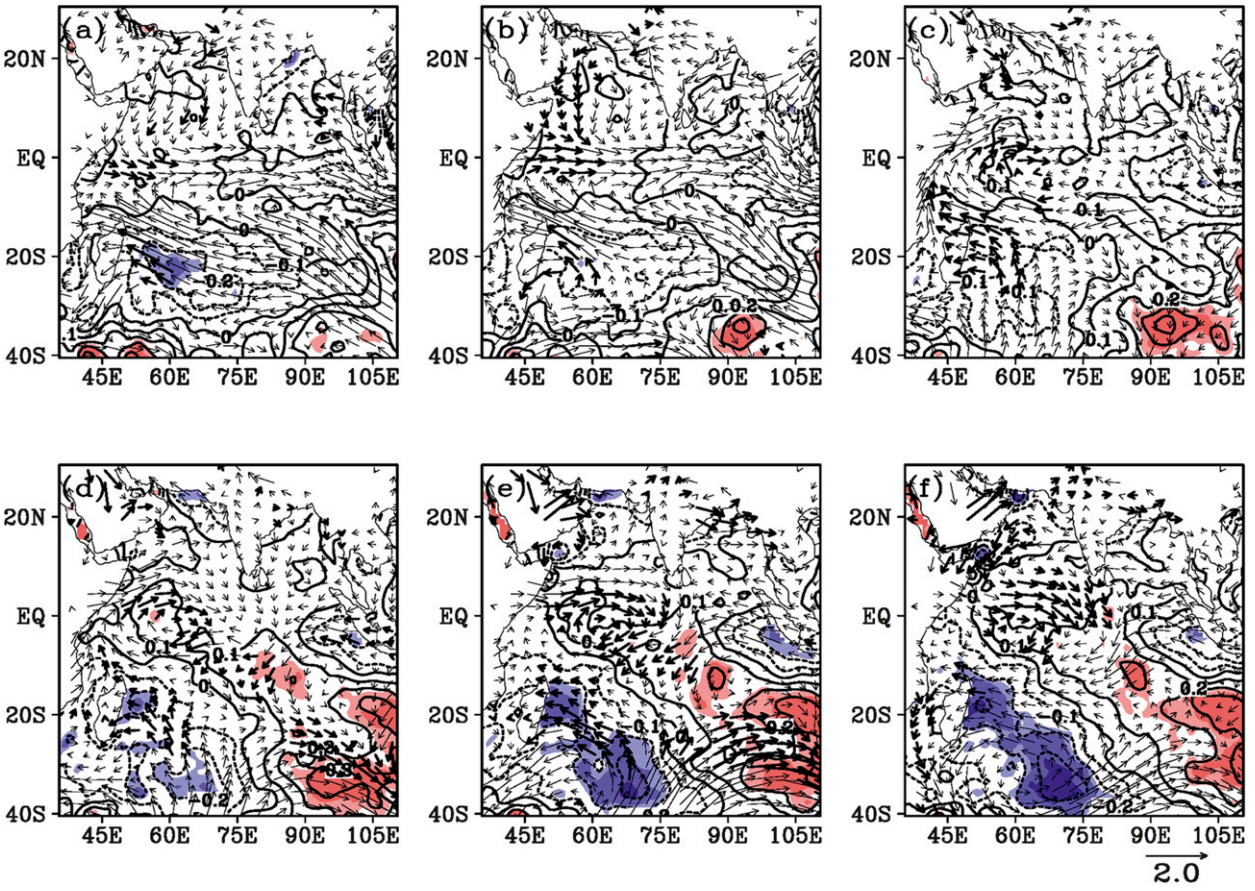

FIG. 10. As in Fig. 9, but for negative SIOD-like years.

over the western tropical Indian Ocean. The associated lower-tropospheric convergence may cause divergence over the tropical Indian Ocean and convergence over the Arabian Sea. That convergence may induce easterly anomalies of the divergent wind component off the eastern coast of the BOB. The divergence over the tropical Indian Ocean may enhance the interhemispheric vertical circulation and generate descending motion over the same region and cyclonic anomalies over the Indian peninsula. The combined effect of the divergent and rotational wind anomalies and enhanced interhemispheric vertical circulation facilitates easterly anomalies and weakens the climatological water vapor flux from the northern BOB to the LLH. Therefore, anomalous water vapor divergence and less precipitation are observed over the LLH. During negative SIOD-like summers, positive SST anomalies in the tropical Indian Ocean may suppress the interhemispheric vertical circulation via enhanced tropical convection in the Southern Hemisphere and lower-tropospheric divergence in the Northern Hemisphere. Accordingly, an anticyclonic anomaly is induced over the BOB, which in turn results in anomalous water vapor convergence and increased precipitation over the LLH. In this case, the divergent wind component is weak and rotational component dominant. The summer precipitation anomalies around the Indian subcontinent also contribute constructively to the current LLH precipitation anomalies to a certain degree. Further analyses indicate that the summer SIOD-like pattern can be traced to preceding seasons, especially in positive SIOD-like years. The SST–wind–evaporation feedback mechanism could account for the maintenance of the SIOD-like pattern, and oceanic advection may also contribute.

Earlier studies suggested a seesaw relationship between the Indian summer monsoon and LLH summer rainfall. When that monsoon is active, two cyclonic circulations are observed, over the Arabian Sea and BOB, and the monsoon trough traverses central India. During this time, divergent flow controls the LLH and induces below normal rainfall there. When the Indian summer monsoon breaks off, opposite climate anomalies are observed (e.g., Zhou and Xu 1981; Chen et al. 1984). Some recent work indicates that a warm south Arabian Sea and

BOB, together with a cold southeastern Indian Ocean, favor abundant rainfall over India (Boschat et al. 2012; Nayagam et al. 2012). These results are compatible with the present conclusion, suggesting that the circulation anomalies over the BOB are the major factors through which the SIOD-like SST anomalies influence summer rainfall extremes over the LLH.

The effect of the Indian Ocean on summer monsoon rainfall over eastern China has been shown by many studies (e.g., Li et al. 2008; Xie et al. 2009; Huang et al. 2010). In our study, its effect on LLH summer rainfall was investigated based on observational and reanalysis data. The identified influences of the SIOD-like SST pattern are stronger than that of ENSO reported in Liu et al. (2011). The SIOD-like pattern is characterized by both more stations and higher confidence levels than those associated with the ENSO pattern. To our knowledge, the present results are the best that have ever been reported for variations of LLH summer rainfall. Moreover, the positive SIOD-like patterns in 2009, 2010, and 2011 reasonably account for the consecutive droughts over the LLH in those years to a large degree, which may not be explained by ENSO. On the other hand, the SIOD-like pattern is intrinsic and partially independent of ENSO (e.g., Behera and Yamagata 2001; Wang et al. 2003; Morioka et al. 2012). That pattern can be observed several months before summer. Hence, it may be used as a potential predictor for summer rainfall in the LLH, especially during a positive SIOD-like phase.

One may argue that the results reported in this paper are mainly on the decadal time scale because the selected positive and negative SIOD-like years seem to have some decadal distribution (first paragraph of section 4). Hence, a 3–7-yr filtering was applied to all the data to extract the interannual components. Then the same analyses were performed to this 3–7-yr filtered data. It reveals that the interannual component accounts for 40.8% of the total variance. Composite analyses based on the interannual component are almost identical to those based on raw data (figure omitted). So, the results presented in this study are mainly not on the interdecadal time scale but on the interannual time scale. Nevertheless, the linkage between the Indian Ocean and the summer rainfall over LLH is also an interesting issue and it deserves further study in the future.

Acknowledgments. We thank the three anonymous reviewers for their valuable comments that lead to improvement of the manuscript. This work was supported by the National Natural Science Foundation of China (U0933603 and 41230527) and the Science Foundation of Yunnan Province (2009CC002).

REFERENCES

Barriopedro, D., C. M. Gouveia, R. M. Trigo, and L. Wang, 2012: The 2009/10 drought in China: Possible causes and impacts on vegetation. *J. Hydrometeor.,* **13,** 1251–1267.

Behera, S. K., and T. Yamagata, 2001: Subtropical SST dipole events in the southern Indian Ocean. *Geophys. Res. Lett.,* **28,** 327–330.

Boschat, G., P. Terray, and S. Masson, 2012: Robustness of SST teleconnections and precursory patterns associated with the Indian summer monsoon. *Climate Dyn.,* **38,** 2143–2165, doi:10.1007/s00382-011-1100-7.

Bretherton, C. S., C. Smith, and J. M. Wallace, 1992: An intercomparison of methods for finding coupled patterns in climate data. *J. Climate,* **5,** 541–560.

Cao, J., J. M. Hu, and Y. Tao, 2012: An index for the interface between the Indian summer monsoon and the East Asian summer monsoon. *J. Geophys. Res.,* **117,** D18108, doi:10.1029/2012JD017841.

Chen, L. X., S. H. Luo, and R. G. Shen, 1984: The Asian summer monsoon and its relations to the rainfall in China. *Adv. Atmos. Sci.,* **1,** 263–276.

Chen, W., 2002: Impacts of El Niño and La Niña on the cycle of the East Asian winter and summer monsoon (in Chinese). *Chin. J. Atmos. Sci.,* **26,** 595–610.

——, L. H. Kang, and D. Wang, 2006: The coupling relationship between summer rainfall in China and global sea surface temperature (in Chinese). *Climatic Environ. Res.,* **11,** 259–269.

Cheng, J. G., H. M. Yan, and H. S. Yan, 2009: *Analysis on Characteristic and Cause of Severe Climate Disaster in Yunnan* (in Chinese). China Meteorology Press, 250 pp.

Ding, Y., and J. C. L. Chan, 2005: The East Asian summer monsoon: An overview. *Meteor. Atmos. Phys.,* **89,** 117–142.

Fauchereau, N., S. Trzaska, Y. Richard, P. Roucou, and P. Camberlin, 2003: Sea-surface temperature co-variability in the southern Atlantic and Indian Oceans and its connections with the atmospheric circulation in the Southern Hemisphere. *Int. J. Climatol.,* **23,** 663–677, doi:10.1002/joc.905.

Gill, A. E., 1980: Some simple solutions for heat-induced tropical circulation. *Quart. J. Roy. Meteor. Soc.,* **106,** 447–462.

Huang, B., and J. Shukla, 2007: Mechanisms for the interannual variability in the tropical Indian Ocean. Part II: Regional processes. *J. Climate,* **20,** 2937–2960.

Huang, G., K. Hu, and S.-P. Xie, 2010: Strengthening of tropical Indian Ocean teleconnection to the northwest Pacific since the mid-1970s: An atmospheric GCM study. *J. Climate,* **23,** 5294–5304.

Huang, R. H., J. L. Chen, L. Wang, and Z. D. Lin, 2012a: Characteristics, processes, and causes of the spatio-temporal variabilities of the East Asian monsoon system. *Adv. Atmos. Sci.,* **29,** 910–942, doi:10.1007/s00376-012-2015-x.

——, Y. Liu, L. Wang, and L. Wang, 2012b: Analysis of the causes of severe drought occurring in southwest China from the fall of 2009 to the spring of 2010. *Chin. J. Atmos. Sci.,* **36,** 443–457.

Jia, X. L., and C. Y. Li, 2005: Dipole oscillation in the southern Indian Ocean and its impacts on climate. *Chin. J. Geophys.,* **48,** 1323–1335.

Li, S. L., J. Lu, G. Huang, and K. M. Hu, 2008: Tropical Indian Ocean Basin warming and East Asian summer monsoon: A multiple AGCM study. *J. Climate,* **21,** 6080–6088.

Liu, L., R. W. Yang, D. Xing, and J. Cao, 2011: The influence of developing and decaying stages of ENSO on summer precipitation in Yunnan. *J. Trop. Meteor.,* **27,** 278–282.

Lü, J. M., J. H. Ju, J. Z. Ren, and W. W. Gan, 2012: The influence of the Madden-Julian oscillation activity anomalies on Yunnan extreme drought of 2009–2010. *Sci. Chin. Earth Sci.,* **55,** 98–112.

Ma, Y., W. Chen, and L. Wang, 2011: A comparative study of the interannual variation of summer rainfall anomalies between the Huaihe meiyu season and the Jiangnan meiyu season and their climate background (in Chinese). *Acta Meteor. Sin.,* **69,** 334–343.

——, ——, S. Fong, K. Leong, and W. Leong, 2012: Interannual and interdecadal variations of precipitation over eastern China during meiyu season and their relationships with the atmospheric circulation and SST (in Chinese). *Chin. J. Atmos. Sci.,* **36,** 397–410.

Matsuno, T., 1966: Quasi-geostrophic motions in the equatorial area. *J. Meteor. Soc. Japan,* **44,** 25–42.

Morioka, Y., T. Tozuka, and T. Yamagata, 2012: How is the Indian Ocean subtropical dipole excited? *Climate Dyn.,* **41,** 1955–1968, doi:10.1007/s00382-012-1584-9.

Nayagam, L. R., J. Rajesh, and H. S. R. Mohan, 2012: The influence of Indian Ocean sea surface temperature on the variability of monsoon rainfall over India. *Int. J. Climatol.,* **32,** 1482–1494, doi:10.1002/joc.3528.

NCC/CMA, 2012: *China Climate Impact Assessment*. National Climate Center/China Meteorological Administration Rep. 4, 19 pp.

Qin, J., J. H. Ju, and M. E. Xie, 1997: *Weather and Climate in Low Latitudes Plateau* (in Chinese). China Meteorology Press, 210 pp.

Rayner, N. A., D. E. Parker, E. B. Horton, C. K. Folland, L. V. Alexander, D. P. Rowell, E. C. Kent, and A. Kaplan, 2003: Global analyses of sea surface temperature, sea ice, and night marine air temperature since the late nineteenth century. *J. Geophys. Res.,* **108,** 4407, doi:10.1029/2002JD002670.

Reason, C. J. C., 2001: Subtropical Indian Ocean SST dipole events and southern African rainfall. *Geophys. Res. Lett.,* **28,** 2225–2227.

Rienecker, M. M., and Coauthors, 2011: MERRA: NASA's Modern-Era Retrospective Analysis for Research and Applications. *J. Climate,* **24,** 3624–3648.

Shen, S. H., and K. M. Lau, 1995: Biennial oscillation associated with the East Asian summer monsoon and tropical sea surface temperature. *J. Meteor. Soc. Japan,* **73,** 105–124.

Song, J., H. Yang, and C. Y. Li, 2011: A further study of causes of the severe drought in Yunnan Province during the 2009/2010 winter. *Chin. J. Atmos. Sci.,* **35,** 1009–1019.

Sun, C., and S. Yang, 2012: Persistent severe drought in southern China during winter–spring 2011: Large-scale circulation patterns and possible impacting factors. *J. Geophys. Res.,* **117,** D10112, doi:10.1029/2012JD017500.

Tao, S. Y., and L. X. Chen, 1987: A review of recent research on the East Asia summer monsoon in China. *Monsoon Meteorology,* C. P. Chang and T. N. Krishnamurti, Eds., Oxford University Press, 60–92.

Tao, Y., J. Cao, J. Hu, and Z. Dai, 2013: A cusp catastrophe model of mid–long-term landslide evolution over low latitude highlands of China. *Geomorphology,* **187,** 80–85, doi:10.1016/j.geomorph.2012.12.036.

Terray, P., P. Delecluse, S. Labattu, and L. Terray, 2003: Sea surface temperature associations with the late Indian summer monsoon. *Climate Dyn.,* **21,** 593–618, doi:10.1007/s00382-003-0354-0.

Wang, B., R. Wu, and T. Li, 2003: Atmosphere–warm ocean interaction and its impact on Asian–Australian monsoon variability. *J. Climate,* **16,** 1195–1211.

Wang, L., and R. Wu, 2012: In-phase transition from the winter monsoon to the summer monsoon over East Asia: Role of the Indian Ocean. *J. Geophys. Res.,* **117,** D11112, doi:10.1029/2012JD017509.

Wang, Z. Y., F. M. Ren, L. Sun, Y. J. Liu, P. L. Wang, J. Y. Tang, D. M. Wang, and D. Li, 2012: Analysis of climate anomaly and causation in summer 2011 (in Chinese). *Meteor. Mon.,* **38,** 448–455.

Washington, R., and A. Preston, 2006: Extreme wet years over southern Africa: Role of Indian Ocean sea surface temperatures. *J. Geophys. Res.,* **111,** D15104, doi:10.1029/2005JD006724.

Xie, M. E., J. G. Cheng, B. Fan, and X. S. Gao, 2005: Diagnosis of high temperature and drought event in summer 2003 in Yunnan. *Meteor. Mon.,* **31,** 32–37.

Xie, S. P., K. Hu, J. Hafner, H. Tokinaga, Y. Du, G. Huang, and T. Sampe, 2009: Indian Ocean capacitor effect on Indo–western Pacific climate during the summer following El Niño. *J. Climate,* **22,** 730–747.

Yan, H. S., Q. Zhang, and W. H. You, 1994: Effect of circulation variation on precipitation in May in Yunnan Province and its long-range forecast. *Plateau Meteor.,* **13,** 217–223.

——, Y. B. Lu, J. G. Cheng, H. Duan, and S. Y. Yang, 2005: The impact of preceding atmospheric circulation and SST variation on flood season rainfall in Yunnan. *J. Trop. Meteor.,* **11,** 121–130.

Yang, J., Q. Liu, S.-P. Xie, Z. Liu, and L. Wu, 2007: Impact of the Indian Ocean SST basin mode on the Asian summer monsoon. *Geophys. Res. Lett.,* **34,** L02708, doi:10.1029/2006GL028571.

——, D. Y. Gong, W. S. Wang, M. Hu, and R. Mao, 2012: Extreme drought event of 2009/2010 over southwestern China. *Meteor. Atmos. Phys.,* **115,** 173–184, doi:10.1007/s00703-011-0172-6.

Yang, Y. L., Y. Du, H. S. Chen, and Y. S. Zhang, 2011: Influence of ENSO event on rainfall anomaly over Yunnan Province and its neighboring regions during late spring-early summer. *Chin. J. Atmos. Sci.,* **35,** 729–738.

Zhou, Y. F., and S. Y. Xu, 1981: The activity of the summer monsoon and rainfall in southwest China in 1979 (in Chinese). *The National Symposium Collections on the Tropical Summer Monsoon,* People's Press, 64–72.